JCBM 1699
26 March 2009 Disk Used
ARTICLE IN PRESS
No. of Pages 8, Model 5G

Construction and Building Materials xxx (2009) xxx–xxx

Contents lists available at ScienceDirect

Construction and Building Materials

journal homepage: www.elsevier.com/locate/conbuildmat

Assessment of the state of conservation of buildings through roof mapping using very high spatial resolution images

Luísa Gonçalves [a,*], Cidália C. Fonte [b,c], Eduardo N.B.S. Júlio [d], Mario Caetano [e,f]

[a] Polytechnic Institute of Leiria, ~~School of Technology and Management~~ Morro do Lena – Alto Vieiro, Apart. 4163, 2411-901 Leiria, Portugal
[b] Institute for Systems and Computers Engineering at Coimbra, Portugal
[c] Department of Mathematics, University of Coimbra, Portugal
[d] ISISE, Civil Engineering Department, University of Coimbra, Portugal
[e] Portuguese Geographic Institute (IGP), Remote Sensing Unit (RSU), Lisboa, Portugal
Q1 [f] CEGI, Instituto Superior de Estatística e Gestão de Informação, ISEGI, Universidade Nova de Lisboa, Portugal

ARTICLE INFO

Article history:
Received 4 September 2008
Accepted 11 March 2009
Available online xxxx

Keywords:
Building roofs
Soft classification
Hybrid classification
Measures of uncertainty
Cultural heritage

ABSTRACT

The assessment of the state of conservation of buildings is extremely important in urban rehabilitation. In the case of historical towns or city centres, the pathological characterization using traditional methods is a laborious and time consuming procedure. This study aims to show that Very High Spatial Resolution (VHSR) multispectral images can be used to obtain information regarding the state of conservation of roofs where, usually, building degradation starts. The study was performed with multispectral aerial images with a spatial resolution of 0.5 m. To extract the required information, a hybrid classification method was developed, that integrates pixel and object based classification methods, as well as information regarding the classification uncertainty. The proposed method was tested on the classification of the historical city centre of Coimbra, in Portugal, that includes over than 800 buildings. The results were then validated with the data obtained from a study conducted during 2 years by a nine element team from the University of Coimbra, using traditional methods. The study performed achieved a global classification accuracy of 78%, which proves that the state of conservation of roofs can be obtained from VHSR multispectral images using the described methodology with a fairly good accuracy.

1. Introduction

Before planning an urban intervention in historical towns or city centres, it is necessary to characterize what exists by performing an architectural and structural survey of buildings within that area [10]. This plays a crucial role in defining the required conservation or rehabilitation operations. Traditional techniques used to identify and map both structural and non-structural anomalies are manually performed and require an individual on-site analysis of each building. These techniques present major drawbacks as they are work-intensive and time consuming [10]. Furthermore, frequently some parts of the buildings such as roofs are inaccessible, which makes the inspection process even more difficult. Therefore, it is necessary to develop new methods, by exploring other possible sources of information, that can provide data on existing anomalies, such as ~~durt~~ deterioration, cracking, biological colonization, moss, and pioneer vegetation, overcoming the disadvantages of traditional methods previously referred to.

Some experimental tests, ~~preformed~~ mainly on stone monuments and masonry walls, proved that it is possible to obtain accurate information about materials and degradations on buildings facades through an automatic classification from visible and near infrared photographs (e.g. [10,12,13,15]). The study reported here intends to evaluate the applicability of Very High Spatial Resolution (VHSR) multispectral aerial images, which have additional problems due to geometric and atmospheric distortions when compared to ground photographs, to detect damages on more than 800 building roofs situated in a historical city centre and to identify their state of conservation. Multispectral aerial images, with a spatial resolution of 0.5 m in four spectral wavebands, which ~~has~~ spatial and spectral characteristics comparable to VHSR satellite images, were used.

Although the VHSR multispectral images have great potential, they also present drawbacks and limitations, such as, the increase of the spectral variability and the amount of shadows, as well as the enormous amounts of data [3]. In addition, although the number of pure pixels increases with the spatial resolution, this increase is followed by the presence of classes that are mosaics of single entities or a spatial arrangement of pixels, such as buildings. There are several available techniques for the automatic extraction

* Corresponding author. Tel.: +351 244 843 339; fax: +351 244 820 310.
E-mail address: luisag@estg.ipleiria.pt (L. Gonçalves).

0950-0618/$ - see front matter © 2009 Published by Elsevier Ltd.
doi:10.1016/j.conbuildmat.2009.03.002

of information from these images. They can be performed on a pixel basis (e.g. [17,2,19,11]) object basis (e.g. [8,3]) or a combination of both (e.g. [18,14]). This last approach has been named as per-field classification when the objects are obtained from digital vector data or Geographic Information Systems (GIS) [1]. Even though, some new approaches have been developed, the efficient extraction of information from VHSR images still remains to impose new demands and the need to develop methodologies that incorporate shape and context, which are some of the main clues used by a human interpreter, and a closer integration of remote sensing and GIS [4,3].

In this study a hybrid classification method is developed to obtain information about the buildings roof materials and their pathologies. The method combines pixel and object classification and incorporates uncertainty information in the soft automatic classification of the images. This approach has similarities with the per-field classification since the objects used in the classification process were obtained from a vector cartographic map of the region. The results are then compared with the ones obtained with a traditional pathology survey, conducted during 2 years by a nine element team from the University of Coimbra, and some conclusions are drawn.

2. Data set and case-study area

The case-study area selected is the historical city centre of Coimbra, in Portugal, with an area of approximately 14.8 ha, that includes over than 800 buildings, some of them are historical buildings, colleges and monasteries, most of these from the 16th century, innumerable alleyways and small squares (Fig. 1).

In the study herein described, ~~we used~~ multispectral aerial images with a resolution of 0.5 m, which belong~~s~~ to a set of ortho rectified digital images covering the Portuguese mainland territory, obtained by plane between 2005 and 2006 with an UltraCam™ sensor of Vexcel by the Portuguese Geographic Institute (IGP) and the Portuguese Forest Services (DGRF). The study was performed using four multispectral bands (blue, green, red and near infrared) and the pixels are recorded in eight bits. A vegetation index was also computed for each data image, namely the Normalized Difference Vegetation Index (NDVI, Eq. (1)) which was used as additional band information to improve the detection of areas with chlorophyll (e.g. moss, lichen, moulds).

$$\mathrm{NDVI} = (\rho_{\mathrm{nir}} - \rho_{\mathrm{red}})/(\rho_{\mathrm{nir}} + \rho_{\mathrm{red}}) \tag{1}$$

where ρ_{nir} and ρ_{red} represent the surface reflectance of near infrared and red bands, respectively.

A vector cartographic map, at the 1:1000 scale, was used to obtain the polygons corresponding to the buildings of the case-study area (Fig. 1). The buildings information was extracted from the cartography and imported to a GIS.

3. Proposed method

Multispectral classification methods are based on the fact that the reflectance characteristics of the different land cover classes depend upon the radiation wavelength. The representation of the intensity values registered at each pixel for n image channels (corresponding to n different wavelengths) into an n-dimensional feature space generates a cluster, in this n-dimensional space, for each class. In the supervised classification methods, reference areas are used to identify and mark this clusters.

In this study, a previous analysis, by visual interpretation, of the images ~~were~~ made to evaluate if it was possible to identify the main materials existing in the area, the presence of pathologies in the buildings roofs and, when present, the different ~~kind~~ of pathologies. It was possible to conclude that, even though the images have very high spatial resolution, these only enable the identification of the roofs with pathologies and do not allow the identification of their different types. Besides that, the majority of roofs have several types of pathologies, which makes the definition of the reference (or training) areas, which are used to perform the classification and validation, considerably difficult, even with 0.5 m pixel spatial resolution. This previous analysis was followed by the ~~definition~~ of the method, the definition of classes and the identification of reference areas.

The main roof materials in the case-study area are: ceramic tiles; fibrocement corrugated sheets; and steel panels. The results obtained by the survey performed by the University of Coimbra revealed that, from the 681 buildings studied (82% of the buildings of the case-study area), 90% have ceramic tile roof materials. For this reason, the present study focuses only in the identification of buildings with ceramic tile roof pathologies, to obtain a Building Pathology Map (BPM). The extraction of this kind of information from the image requires, not only the classification of the elementary entities (pixels in this case), but also the analysis of their distribution inside the buildings. To achieve this goal, an independent identification of the roof materials, such as ceramic roof tile and steel roof panel, was made, producing the information about the

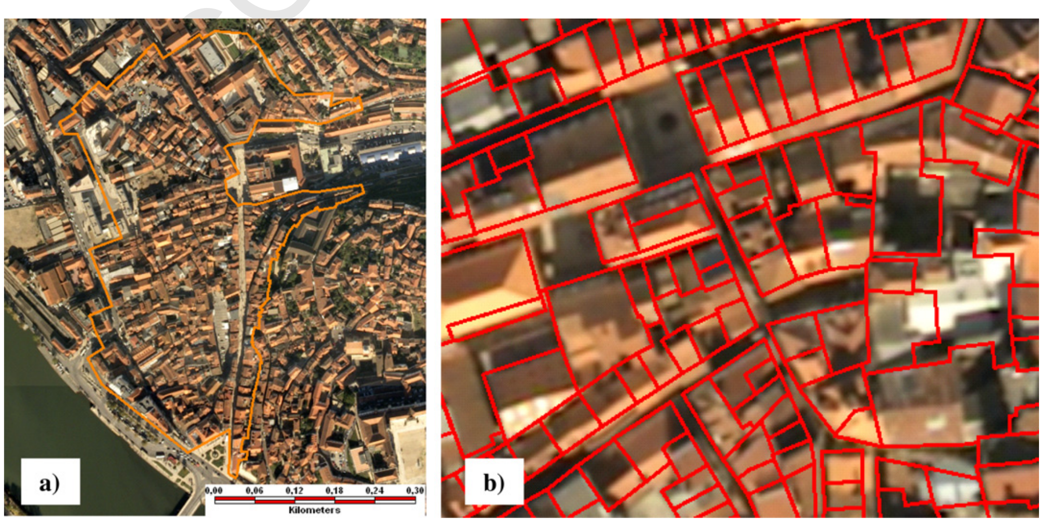

Fig. 1. The data of the case-study area: (a) aerial images (RGB321); (b) overlay of the vector buildings map and the aerial images.

Surface Elements Material (SEM). The same approach was used to identify the parts of buildings that present any kind of pathology, producing the information about the Surface Elements Pathology (SEP). The classification method developed is a hybrid approach that includes two preliminary pixel classifications of the image, constructing a Surface Elements Materials Map (SEMM) and a Surface Elements Pathology Map (SEPM), based on a soft probabilistic pixel classification. This classification method assigns, to each pixel, different degrees of probability to the several classes under consideration. This extra data provided additional information at the pixel level which allowed the assessment of the classification uncertainty.

Since the survey used as reference information produced a classification of the buildings conservation level, to allow the comparison of the results obtained with both approaches, it was crucial that the results produced with this new approach would also be at the building level. Therefore, the subsequent step was the identification of the Building Units (BU), which ~~was~~ obtained from the vector cartographic map available at 1:1000 scale. This information was converted to the raster format, generating a raster buildings map, and was used as a mask, so that only the parts of the classified image inside the buildings were processed to obtain the BPM. At this stage, the BU becomes the basic units rather than the individual pixels. The pathologies identification within each BU was performed considering a set of rules that included information about: (1) the distribution of the classified pixels; (2) the probabilities assigned to the several classes for each pixel; (3) the degree of uncertainty associated ~~to~~ these assignments. The introduction of uncertainty information, associated ~~to~~ the pixel classification of SEP and the SEM, was used to avoid the use of misclassified pixels in the transformation from the SEMM and the SEPM to the BPM, since it was shown that this approach improves the land cover classification [9].

The proposed method includes the following steps (see Fig. 2): (1) soft pixel based classification of the multispectral aerial image to obtain the SEMM and the SEPM; (2) evaluation of the classification; (3) evaluation of the classification uncertainty; (4) pathology classification of the buildings with ceramic tile material, based on decision rules using the SEMM the SEPM and their uncertainty information; (5) evaluation of the classification accuracy.

3.1. Training and testing data

The sampling design has an important role in the classification and accuracy assessment. In this study five sampling protocols were established. Two for training, respectively, the SEP and the SEM pixel classification, two to evaluate these classifications and another to evaluate the final building map classification. The training dataset consisted on a semi-random selection of sites (Fig. 3). For each class, fifteen building polygons were selected manually from the case-study area and a stratified random selection of 100 samples inside the chosen buildings was performed. To evaluate the soft pixel classification accuracy a stratified random sample of 100 pixels per class was made, spread over all buildings. This number of pixels was used because it is recommended to obtain a standard error of 0.05 for the estimated user's accuracy of each class [16]. The soft pixel classification was only evaluated inside the building polygons. For the accuracy assessment of the final BPM a stratified random selection of 100 samples was performed considering all buildings. The accuracy assessment was made with

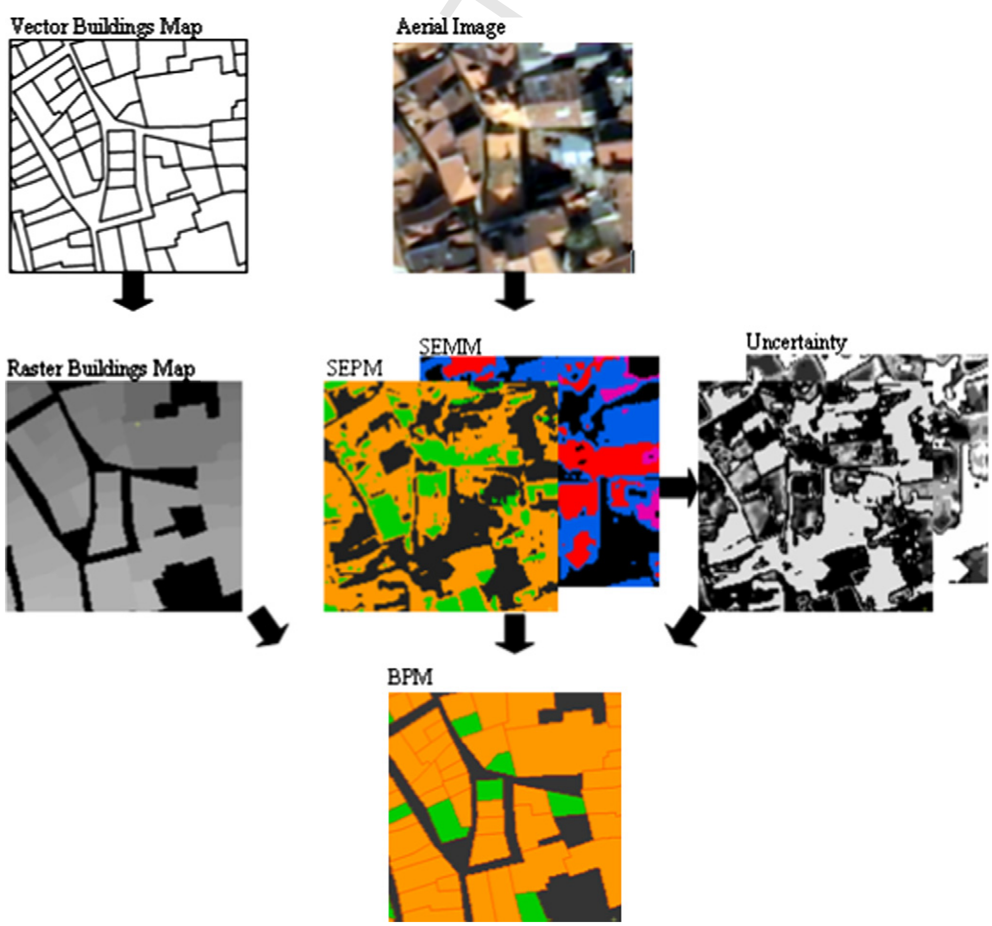

Fig. 2. Flowchart of the method.

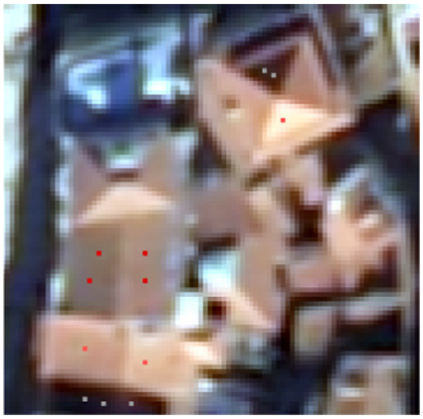

Fig. 3. Example of sample training areas in the aerial images RGB321.

an error matrix. In this stage, the survey performed by the University of Coimbra regarding all buildings was used as reference information to identify the ceramic building roofs with anomalies and not deteriorated in the case-study area.

3.2. Spectral analysis

The information of the training data set was also used to study the spectral separability of the classes at the pixel level. For this purpose the Bhattacharya Distance (B-Distance) and a dimensional scatter plot were used.

To visualize the results the red and the near infrared bands were used as axis, since, due to the presence of vegetation and patches in some roofs, these two bands are the ones that better allow the differentiation between the classes. The B-Distance can serve as an indicator to the final performance of the supervised classification. A high B-Distance value means that classes are spectrally separable, therefore, the larger the B-Distance value the better the final classification.

3.3. Classification

The classification method includes several steps. First, two soft pixel classifications of the image were performed using a probabilistic classifier based on Bayesian modelling, for the identification and mapping of the SEP and the SEM. This classifier was selected because it has been used in other studies to derive accurate classifications (e.g. [2,19,5]). The Bayesian classifier is similar to the Maximum Likelihood Classifier (MLC), the most widely used image classifier in remote sensing, but it has been mainly used in its crisp version. However, the output may be derived in the form of posterior class probabilities providing a soft classification (e.g. [17,6,7]). Unlike traditional hard classifiers, the output is not a single classified map, but rather a set of images (one per class) that express the probability that each pixel belongs to the class in question. This extra data also provided additional information at the pixel level which allowed the assessment of the classification uncertainty. The soft pixel classification of the SEM was driven using four multispectral bands and the SEP was performed also with the NDVI vegetation index.

The surface elements classes used in this study for the SEMM were "Dark Ceramic Roof Tile" (CT-D), "Bright Ceramic Roof Tile" (CT-B) "Fibrocement Corrugated Roof Sheet" (FC), "Steel Roof Panel" (SP) and "Roof Shadow" (RS). For the SEPM the classes were "Ceramic Roof Tile Anomalies" (C-A), "Ceramic Roof Tile Not Deteriorated" (C-ND) and Ceramic Roof tile with Shadow (C-S). The Roof Shadow and Ceramic Roof tile with Shadow classes were considered due to the significant amount of shadows that the VHSR multispectral aerial images presented. By considering these classes in the development of classification rules it was possible to reduce misclassification of roof materials and pathologies at the building level.

Secondly, the uncertainty of the probabilistic classification was evaluated using an indicator of the Classification Uncertainty (CU), available in the commercial software IDRISI~~S~~, given by

$$CU = 1 - \frac{\max\limits_{i=1,\ldots,n}(p_i) - \frac{\sum_{i=1}^{n} p_i}{n}}{1 - \frac{1}{n}} \qquad (2)$$

where p_i $(i = 1, \ldots, n)$ are the probabilities associated ~~to~~ the several classes and n is the number of classes under consideration. This indicator assumes values in the interval [0, 1] ~~and only depends on: the maximum probability; the sum of all probabilities assigned to the class; the total number of classes~~. CU evaluates until which point the classification is dispersed over more than one class and the degree of compatibility with the most probable class, providing information regarding the classifier difficulty in assigning only one class to each pixel.

The subsequent step was the construction of the BPM through the combination of the SEPM, the SEMM, their uncertainty information and the buildings polygons converted to the raster format and used as a mask. This was achieved through ~~a~~ development of rules that incorporate the arrangement of the previous soft pixel based classifications within each BU, the information on the probabilities assigned to the several classes at each pixel and the degree of uncertainty associated ~~to~~ these assignments. The rules construction requires a preliminary analysis of the probabilities assigned to the SEP and SEM classes and their uncertainty in order to choose the appropriate thresholds. The BU classes used in this study are: "Buildings with Ceramic Roof Tile With Anomalies"(B-C-A), varying from "State of Conservation 1" (SC1) to "State of Conservation 4" (SC4); and "Buildings With Ceramic Roof Tile Not Deteriorated" (B-C-ND), corresponding to "State of Conservation 5" (SC5).

The transformation of a SEPM and a SEMM into a BPM is similar to a decision tree which, for geographical objects, is a hierarchical structure consisting of several levels. At each level a test is applied to one or more attribute values. ~~Application~~ of ~~the~~ rule results either into a leaf, allocating an object to a class, or a new decision node, specifying ~~a further~~ decision rule. Fig. 4 shows the BU classes classification workflow and Table 1 shows the used rules. The aim of rules 1–3 is to make a distinction between 'Buildings With Ceramic Roof Tile' (B-C) and 'Buildings With No Ceramic Roof Tile' (B-NC). ~~Rule~~ 4–6 classifies the 'Buildings With Ceramic Roof Tile' into "Buildings With Ceramic Roof Tile With Anomalies" and "Buildings With Ceramic Roof Tile Not Deteriorated", corresponding to "State of Conservation 5". Rule 7 assigns the "Buildings With Ceramic Roof Tile With Anomalies" (B-C-A) to one of four possible classes: "State of Conservation 1", "State of Conservation 2", "State of Conservation 3" and "State of Conservation 4".

4. Results and discussion

4.1. Spectral analysis

Figs. 5 and 6 show the spectral separability of, respectively, the SEM and SEP classes. It can be observed that, for the represented wavelengths, the ellipses corresponding to all SEM and SEP classes are almost completely separated. Only some minor overlap is observed, mainly between Roof Shadows (RS) and the classes Fibrocement Corrugated Roof Sheet (FC) and Dark Ceramic Roof Tile (CT-D). Ceramic Roof Tile with Shadows (C-S) spectral signature also presents a slight overlap with the class Ceramic Roof Tile with

Please cite this article in press as: Gonçalves L et al. Assessment of the state of conservation of buildings through roof mapping using very high spatial resolution images. Constr Build Mater (2009), doi:10.1016/j.conbuildmat.2009.03.002

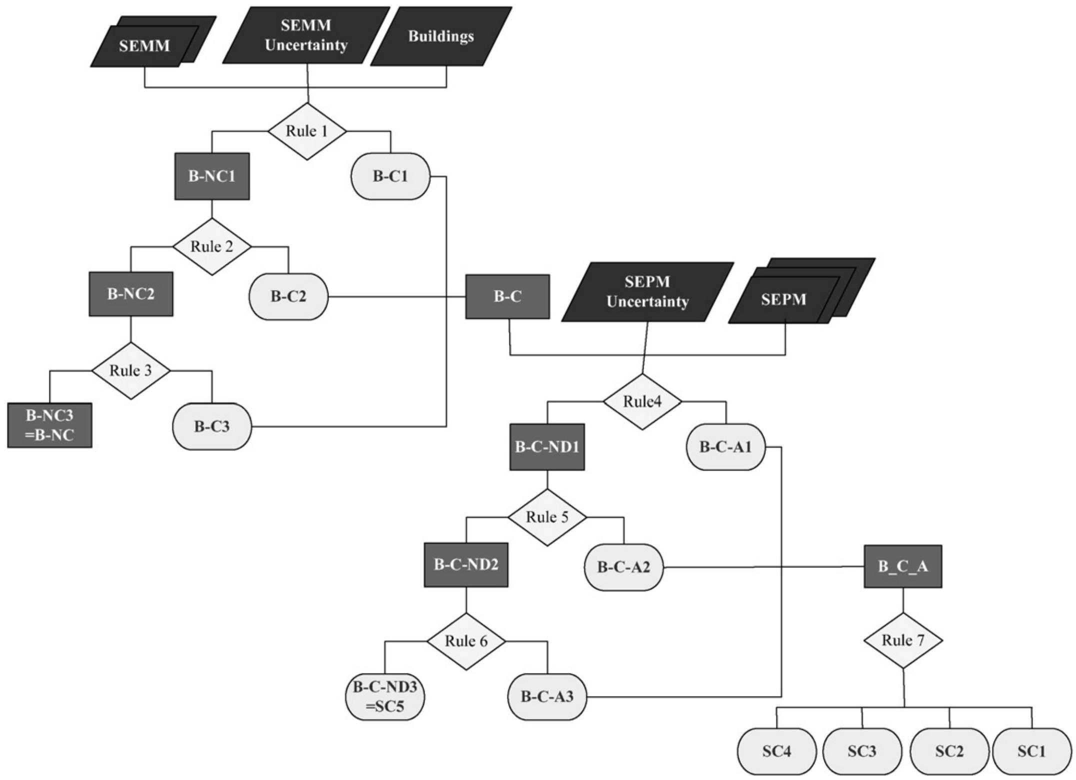

Fig. 4. Building unit classes classification workflow.

Anomalies (C-A). The results given by the B-Distance reinforce the results shown by the scatter plot. The average separability measure of the SEMM classes is 1.87 and for the SEPM the average separability is 1.93 indicating a good performance of the supervised classification.

4.2. Classification

The accuracy of the SEMM and SEPM produced is presented in Table 2, expressed by the Global Accuracy (GA) and the Kappa coefficient. The accuracies of the SEMM and the SEPM obtained are very similar, but the SEPM one is slightly better, which is consistent with the B-Distance results. The User's and Producer's accuracy of the SEMM and SEPM are presented, respectively, in Figs. 7 and 8.

The ~~Users~~ and Producer's accuracy values per class show that the class Ceramic Roof Tile (CT) was very well identified. Some confusion was observed between Fibrocement Corrugated Roof Sheet (FC), Steel Roof Panel (SP) and Roof Shadow (RS), which lowered the respective accuracy specific indices. This confusion was due to the proximity of the corresponding spectral signatures.

Table 1
Classification rules.

Rule Number	Rules	If true
1	At least 50% of the pixels of the SEMM, located inside the BU, are classified as "Ceramic Roof Tile" with a probability higher than 0.75 and uncertainty less than 0.25.	Assign to class B-C
2	If the percentage of "Ceramic Roof Tile", with a probability higher than 0.75 and uncertainty less than 0.25, inside the BU, is higher than the percentage of "Fibrocement Corrugated Roof Sheet" and "Steel Roof Panel" and higher than the percentage of "Roof Shadow".	Assign to class B-C
3	If the percentage of "Ceramic Roof Tile", with a probability higher than 0.75 and uncertainty less than 0.25, inside the BU, is higher than the percentage of "Fibrocement Corrugated Roof Sheet" and "Steel Roof Panel" and the percentage of "Roof Shadow is higher than 0,5.	Assign to class B-C
4	At least 50% of the pixels of the SEPM inside the BU classified as "Buildings With Ceramic Roof Tile", is " Ceramic Roof Tile With Anomalies" with a probability higher than 0.75 and uncertainty less than 0.25.	Assign to class B-C-A
5	If the percentage of " Ceramic Roof Tile With Anomalies" inside the BU classified as "Buildings With Ceramic Roof Tile" is higher than the percentage of "Ceramic Roof Tile Not Deteriorated" and higher than the percentage of "Roof Shadow".	Assign to class B-C-A
6	If the percentage of " Ceramic Roof Tile With Anomalies" inside the BU classified as "Buildings With Ceramic Roof Tile" is higher than the percentage of "Ceramic Roof Tile Not Deteriorated" and the percentage of "Roof Shadow" is higher than 0.5.	Assign to class B-C-A
7	Buildings classified as "Buildings with Ceramic Roof Tile With Anomalies" have more than 75% of pixels classified as "Ceramic Roof Tile With Anomalies" with a probability higher than 0.75 and uncertainty lower than 0.25.	SC1
	Buildings classified as "Buildings with Ceramic Roof Tile With Anomalies" have between 50% and 75% of pixels classified as "Ceramic Roof Tile with Anomalies" with a probability higher than 0.75 and uncertainty lower than 0.25.	SC2
	Buildings classified as "Buildings with Ceramic Roof Tile With Anomalies" have between 25% and 50% of pixels classified as "Ceramic Roof Tile With Anomalies" with a probability higher than 0.75 and uncertainty lower than 0.25.	SC3
	Buildings classified as "Buildings with Ceramic Roof Tile With Anomalies" have between 0% and 25% of pixels classified as "Ceramic Roof Tile With Anomalies" with a probability higher than 0.75 and uncertainty lower than 0.25.	SC4

Please cite this article in press as: Gonçalves L et al. Assessment of the state of conservation of buildings through roof mapping using very high spatial resolution images. Constr Build Mater (2009), doi:10.1016/j.conbuildmat.2009.03.002

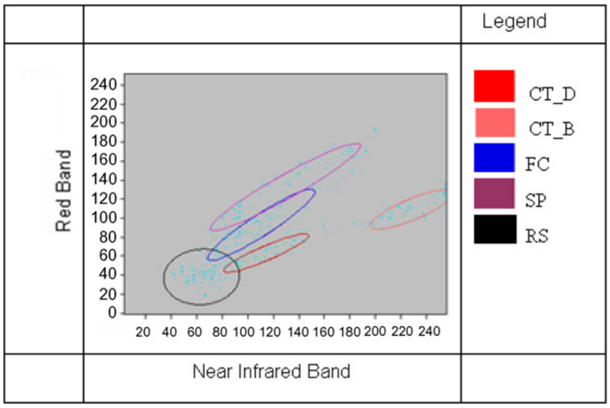

Fig. 5. Spectral separability of the Surface Elements Materials classes: Dark Ceramic Roof Tile (CT-D); Bright Ceramic Roof Tile (CT-B); Fibrocement Corrugated Roof Sheet" (FC); Steel Roof Panel (SP) and Roof Shadow (RS).

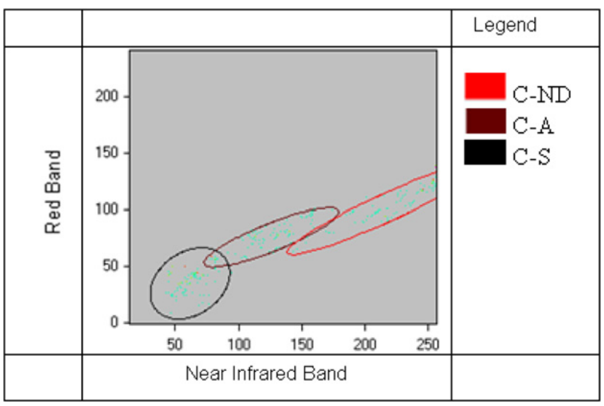

Fig. 6. Spectral separability of the Ceramic Roof Tile with Anomalies (C-A), Not Deteriorated (C-ND) and Ceramic Roof Tile with Shadows (C-S).

Table 2
Classification accuracy indexes.

	GA (%)	Kappa (%)
SEMM	89	86
SEPM	94	92

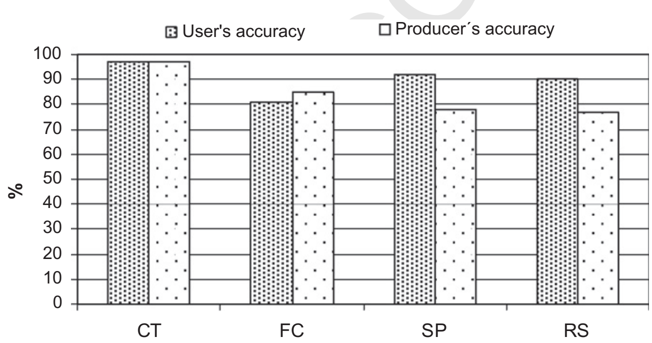

Fig. 7. User's and Producer's accuracy of the Surface Elements Material Map (SEMM) classes: Ceramic Roof Tile (CT), Fibrocement Corrugated Roof Sheet (FC), Steel Roof Panel (SP) and Roof Shadow (RS).

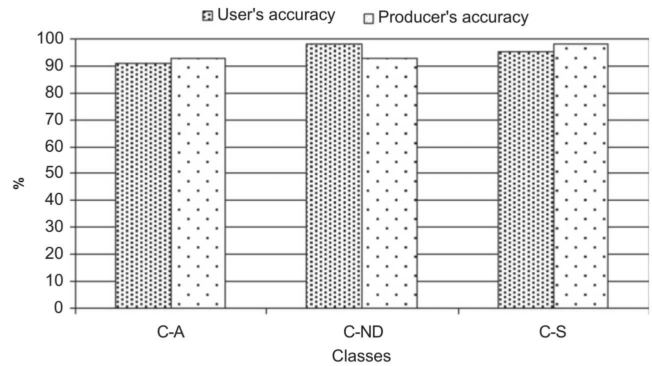

Fig. 8. User's and Producer's accuracy of the Surface Elements Pathology Map (SEPM) classes: Ceramic Roof Tile with Anomalies (C-A), Not Deteriorated (C-ND) and Ceramic Roof Tile with Shadows (C-S).

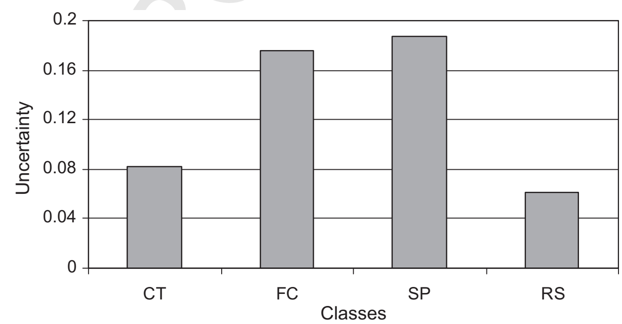

Fig. 9. Average classification uncertainty per class of the surface elements material map.

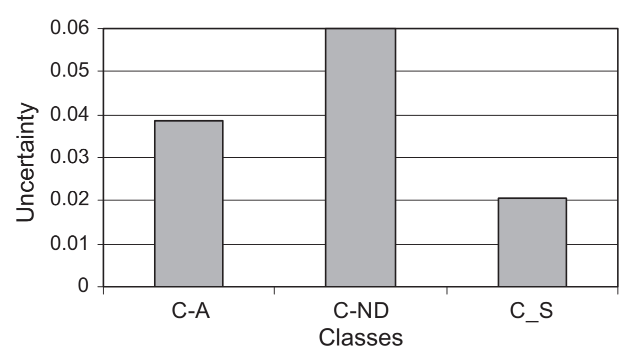

Fig. 10. Average classification uncertainty per class of the surface elements pathology map.

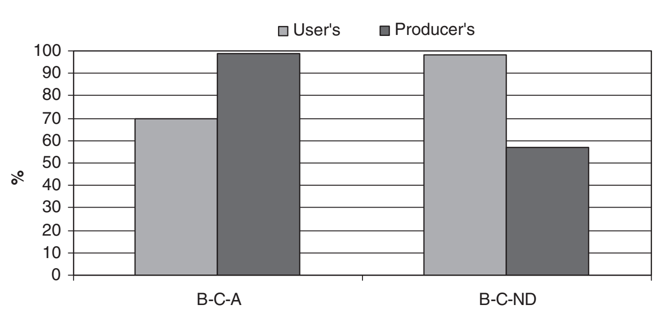

Fig. 11. The User's and Producer's accuracy of the BPM obtained with the hybrid approach applied to the aerial images.

Fig. 8 shows that the classification of Ceramic Roof Tile With Anomalies (C-A) presents higher values for the Producer's accuracy

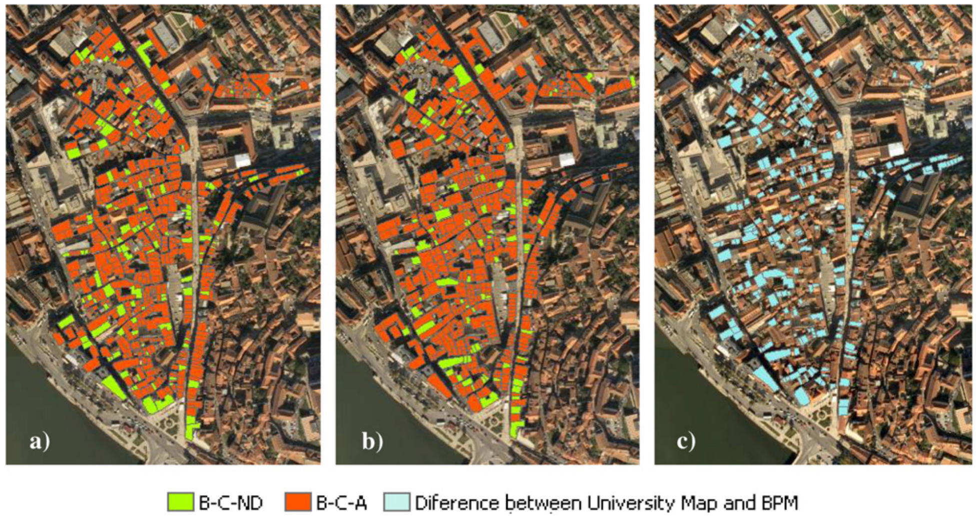

Fig. 12. Comparison between the Building Pathology Map (BPM) and the map made with the traditional approach: (a) Pathology map generated with traditional methods; (b) BPM; (c) difference between the two maps.

than for the User's accuracy while the opposite occurs for the Ceramic Roof Tile Not Deteriorated (C-ND), which means that the C-A class presents more commission errors and the C-ND presents more omission errors.

Figs. 9 and 10 show the average uncertainty per class of the SEMM and SEPM, respectively. The comparison of these results with Figs. 7 and 8 show that they are consistent. For example, the classes Ceramic Roof Tile (CT) and Steel Roof Panel (RS) in the SEMM present the lower values of uncertainty and the higher values of accuracy, while the other two classes show higher uncertainty and lower accuracy.

The global classification accuracy of the BPM was 78%. The User's and Producer's accuracy are shown in Fig. 11. Since the class Buildings With Ceramic Roof Tile With Anomalies (B-C-A) presents lower User's Accuracy it has more commission errors while the class Buildings With Ceramic Roof Tile Not Deteriorated (B-C-ND) has more omission errors (corresponding to lower Producer's Accuracy). This means that some buildings, which were classified with this approach as having anomalies, according to the reference study do not present them.

The reference study analyzed 826 buildings within the case-study area. With this traditional survey, 75% of the buildings were identified as having ceramic roof tile while, with the new approach, 76% of the buildings were identified to have this type of roof, corresponding to a slight increase in the identification of this roof material. The comparison between the two methods showed that 85% of the buildings with ceramic roof tile identified by the traditional survey were also identified with this new approach. In addition, the comparison between the BPM and the map made with the traditional method showed that 77% of the ceramic roof tile with pathologies, identified with the traditional survey was also identified by this new approach (Fig. 12).

The analysis of the differences between the pathology map obtained with the traditional methods and BPM leads to the conclusion that they are mainly due to the presence of shadows in the image, to the fact that the image and the vector cartographic map do not match perfectly (as shown in Fig. 1) and mainly because the traditional survey was made between 2003 and 2004 and the aerial images were produced from aerial digital photos obtained between 2005 and 2006.

Since the shadows spectral signature presents some overlap with the class Ceramic Roof Tile With Anomalies (C-A), some buildings with a great amount of shadows may be wrongly classified as presenting anomalies, which may explain the amount of commission and omission errors shown in the B-C-A and B-C-ND classes (see Fig. 11). The mismatches between the buildings in the vector cartographic map and the image have the consequence that some pixels placed inside the regions corresponding to the buildings actually do not represent parts of buildings and therefore may generate wrong conclusions. Since there is a temporal discrepancy between the data used in both studies some changes occurred in the region, and therefore the different results obtained with both studies for some building may actually be both correct. For example, between these two periods several roofs were repaired or replaced

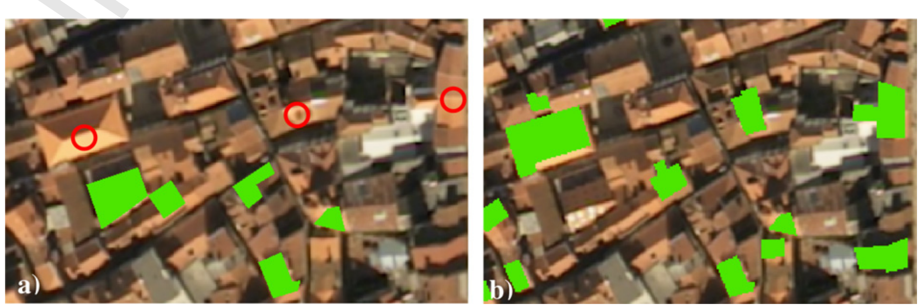

Fig. 13. (a) Extract of the aerial images (RGB321) overlaid with the buildings with ceramic roof tile not deteriorated obtained with the traditional methods. (b) Extract of the aerial images (RGB321) overlaid with the buildings with ceramic roof tile not deteriorated classified by the new approach. The circles mark some of the buildings which roofs were repaired or replaced by new ones and were correctly identified with the new classification approach.

Please cite this article in press as: Gonçalves L et al. Assessment of the state of conservation of buildings through roof mapping using very high spatial resolution images. Constr Build Mater (2009), doi:10.1016/j.conbuildmat.2009.03.002

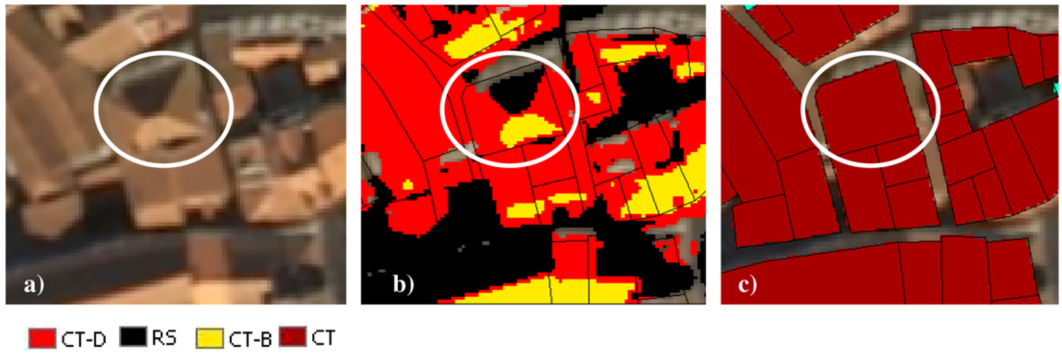

Fig. 14. Transformation of surface elements into building classification units: (a) Extract of the aerial images RGB321; (b) Surface elements pixel classification into "Dark Ceramic Roof Tile" (CT-D), "Bright Ceramic Roof Tile" (CT-B) and Roof Shadow (RS); (c) Building units classification into "Ceramic Tile" (CT) and "Fibrocement Corrugated Roof Sheet or Steel Roof Panel" (FC+SP). The circles mark a building which presented shadows, ~~and~~ bright and dark ceramic roof tile and were correctly identified with this new classification approach.

with new ones, which therefore did not present any anomaly in the aerial images and were well identified with the new classification approach (see Fig. 13). On the other hand some roofs that did not present anomalies in 2003–2004 may have developed some since then, which became visible in 2005–2006.

The increase in VHSR multispectral images spatial resolution, despite enabling the identification of ceramic tile material also allows the identification of other features, such as regions with ceramic tiles that belong to the same roof but present different brightness or shadows due to slope differences and sun orientation. This aspect is a major problem for this kind of application. However, the proposed hybrid method of classification proved to be adequate to solve this kind of difficulties, since it enabled a correct transformation of surface elements into building classification units (see Fig. 14).

5. Conclusions

The obtained results show that the application of very high spatial resolution (VHSR) multispectral images to heritage conservation, in particular to the extraction of information concerning roof anomalies, is very promising. The VHSR image used in the study~~,~~ enabled a good identification of the different roof materials and the presence of their damages. The use of a hybrid pixel-object classification method integrating the surface elements classification uncertainty proved to be valuable and adequate in the classification process to resolve some difficulties found along the study. The global classification accuracy of the Building Pathology Map (BPM) was 78%, and therefore further attention should be given to this approach. From a methodological point of view, the hybrid approach also proved to be adequate for the transformation of surface elements into BPM with a format well suited to be integrated in a GIS.

Acknowledgements

The authors thank the University of Coimbra for providing data related to the state of conservation of buildings in the historical city centre of Coimbra.

References

[1] Aplin P, Atkinson P, Curran P. Per-field classification of land use using the forthcoming very fine spatial resolution satellite sensors: problems and potential solutions. In: Atkinson P, Tate N, editors. Advances in remote sensing and GIS analysis. Chichester: John Wiley and Sons; 1999. p. 219–39.
[2] Atkinson PM, Cutler MEJ, Lewis H. Mapping sub-pixel proportional land cover with AVHRR imagery. Int J Rem Sens 1997;18(4):917–35.
[3] Blaschke T, Burnett C, Pekkarinen A. Image segmentation methods for object-based analysis and classification. In: Jong SM, van der Meer FD, editors. Remote sensing image analysis; 2004. p. 211–34.
[4] Donnay JP, Barnsley M, Longley P. Remote sensing and urban analysis. In: Donnay JP, Barnsley M, Longley P, editors. Remote sensing and urban analysis. New York: Taylor & Francis; 2001. p. 3–18.
[5] Eastman JR, Laney RM. Bayesian soft classification for sub-pixel analysis: a critical evaluation. Photogramm Eng Rem Sens 2002;68:1149–54.
[6] Foody GM. Approaches for the production and evaluation of fuzzy land cover classifications from remotely-sensed data. Int J Rem Sens 1996;17:1317–40.
[7] Foody GM. Sub-pixel methods in remote sensing. In: Jong SM, van der Meer FD, editors. Remote sensing image analysis: including the spatial domain; 2004. p. 37–49.
[8] Gonçalves L, Caetano M. Classificação das imagens do satélite IKONOS utilizando uma abordagem orientada por objectos. In: Bastos L, Matos J, Lidel L, editors. Acta da III Conferência de Cartografia e Geodesia; 2004. p. 287–98.
[9] Gonçalves L, Fonte C, Júlio E, Caetano M. A method to incorporate uncertainty in the classification of remote sensing images. In: Eighth international symposium on spatial accuracy assessment in natural resources and environmental sciences, Shanghai, China; June 2008.
[10] Hemmleb M, Weritz F, Maierhofer C. Damage detection on buildings surfaces with multi-spectral techniques. In: Proc XX CIPA international symposium. Torino: Italy; 2005.
[11] Ibrahim MA, Arora MK, Ghosh SK. Estimating and accommodating uncertainty through the soft classification of remote sensing data. Int J Rem Sens 2005;26:2995–3007.
[12] Lerma JL. Automatic feature recognition technique on stone monuments using visible and IR photography. In: Proc int cultural heritage informatics meeting, vol. 2; 2001. p. 255–8.
[13] Lerma JL. Automatic plotting of architectural facades with multispectral images. J Surv Eng 2005;131(3):77.
[14] Plantier T, Caetano M. Mapas do Coberto Florestal: Abordagem Combinada Pixel/Objecto. In: Bastos L, Matos J, Lidel L, editors. Acta da V Conferência Nacional de Cartografia e Geodesia; 2007. p. 157–66.
[15] Ruiz LA, Lerma JL, Gimeno J. Application of computer vision techniques to suport in the restoration of hitorical buildings. International archives of photogrammetry and remote sensing. Comission III, vol. XXXIV, Part 3A+B; 2002. p. 4.
[16] Stehman SV. Statistical rigor and practical utility in thematic map accuracy assessment. Photogramm Eng Rem Sens 2001;67(6):727–34.
[17] Wang F. Improving remote sensing image analysis though fuzzy information representation. Photogramm Eng Rem Sens 1990;56:1163–9.
[18] Wang L, Sousa WP, Gong P. Integration of object-based and pixel-based classification for mapping mangroves with IKONOS imagery. Int J Rem Sens 2004;20(24):5655–68.
[19] Zhang J, Foody GM. Fully-fuzzy supervised classification of sub-urban land cover from remotely sensed imagery: statistical and artificial neural network approaches. Int J Rem Sens 2001;22:615–28.